MONITORING A-SI:H SOLAR CELLS DEGRADATION BY TWO SIDES BLUE LIGHT COLLECTION

G. Masini*, D. Fischer, J. Hubin, F. Palma* and A. Shah
Institute of Microtechnology, University of Neuchatel
Rue Breguet 2, CH-2000 Neuchatel, Switzerland (fax ++41-38-254276)
*Dipartimento di Ingegneria Elettronica Università 'La Sapienza'
Via Eudossiana, 18 00184 ROMA, Italy (fax ++39 -6-4742647)

ABSTRACT

In view of the persistent lack of correlation between single layer material properties and solar cell performance, one is at present interested in experimental techniques which allow the characterisation of material properties within a full p-i-n cell. In this paper we introduce a novel method to monitor i-layer properties during degradation of a-Si:H p-i-n solar cell. Two blue, strongly absorbed light beams shine from both p- and n- side on the cell, giving rise to an approximately constant density of charge trapped in the deep states over the i-layer. The sign and magnitude of the constant space charge can be systematically varied by the ratio of the two light beams. The deformation in the shape of the built-in electric field within the cell, as induced by this charge, dramatically affects the collection of photogenerated carriers in a very distinctive way. A simple analytical model, based on the 'standard' DOS model for a-Si:H and involving a reduced set of parameters is presented; it allows the determination of the density of the deep defects by fitting experimental collection data. A more detailed modelling of the experiment, using a finite element a-Si:H device simulator, is also presented.

EXPERIMENTAL

The experimental set-up is sketched in Fig.1. An interferential filter (50 nm bandwidth centred on 400 nm wavelength) is used to obtain blue light from a halogen lamp.

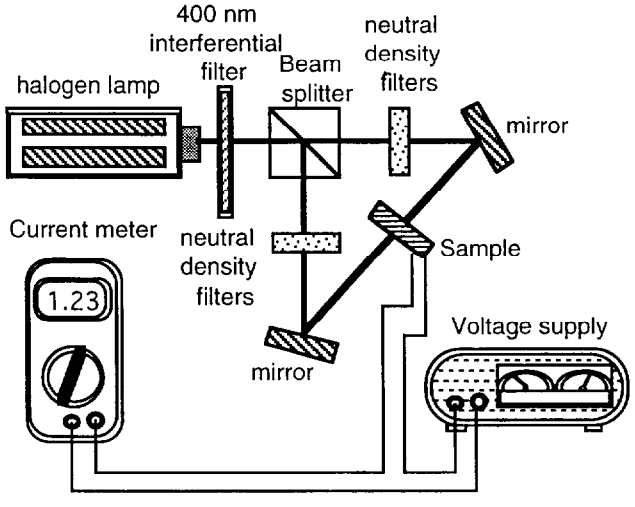

Fig.1: Experimental set-up.

Different light intensities from the two sides are adjusted by interposing neutral density filters.
Experimental data consists of internal collection efficiency values represented as a function of the ratio between the two photocurrents, as generated by each one of the two lights individually (I_{bn}/I_{bp}); I_{bn} and I_{bp} are measured under high reverse bias in order to ensure unity collection. The collection is evaluated as the ratio between the total photocurrent measured at short circuit (I_{sc}) and at high reverse bias (I_{rb}). Each data point consists, thus, of four independent measurements.

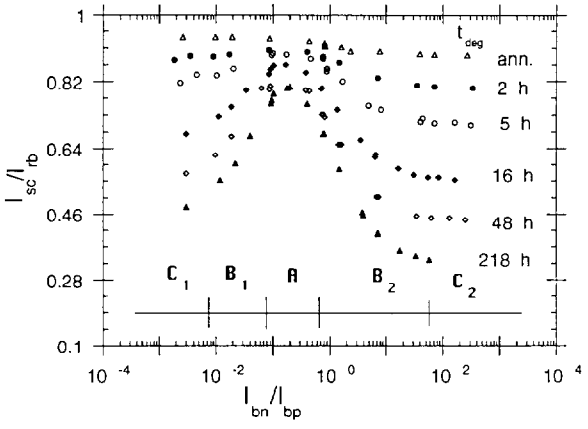

Fig.2: Internal collection at short circuit measured as a function of the relative intensity of the photocurrents generated by blue light shining from n (I_{bn}) and p (I_{bp}) side of the sample.

Samples used are 550 nm thick p-i-n solar cells with a transparent back contact realized by sputtered ITO. A set of measurements is taken in the annealed (2h @ 180 °C) and light-soaked (Sodium Lamp adjusted to give approx. 100 mW/cm^2) states. Experimental results for sample c221193 are reported in Fig.2: different symbols refer to different light soaking times. Clearly, the collection data is a strong function of the degradation time. The main features shown by the curves are: the asymmetric 'bell' shape with the right branch always extended towards lower values of collection, the position of the maximum shifted to the left half plane where the photocurrent generated by light shining from the p-side is stronger and the slopes of the two sides of the 'bell' which increase with increasing degradation. Also the maximum of the curve decreases with increasing degradation.
From a qualitative point of view, strongly absorbed light shining from the p-side is expected to fill the intrinsic layer

CH3365-4/94/0000-0610 $4.00 © 1994 IEEE

with electrons, while holes are injected by the light which enters the n-side. The two populations tend to charge the deep defects and to give rise to a deformation of the built-in electric field. The collection of photogenerated carriers, which in amorphous cells is strongly dependent on the electric field, is expected to have a maximum when the two light beams are adjusted to produce a net zero charge within the intrinsic layer; this corresponds to minimum electric field deformation (region A in Fig.2). On the other side, a strong predominance of electrons produces a net negative charge in the intrinsic layer which, in turn, lowers the electric field in proximity of the p-i interface, thus reducing the collection probability of the photocarriers generated there (region B1). A similar reasoning can be made for excess hole population and electric field at the i-n interface (region B2). The higher the density of deep states, the stronger the electric field quenching for a given ratio of electrons to holes ratio, the smaller the collection probability. Moreover, as long as the tail states are not involved in the space charge, once all deep states are charged no further electric field depression takes place for an increasing unbalance between electrons and holes and collection eventually saturates (regions C1 and C2).

NUMERICAL SIMULATION

With the scope of obtaining a quantitative idea of charge distribution, field deformation and recombination profiles, numerical simulation of the experiment has been performed using the finite elements amorphous silicon device simulator developed at University of Rome. This programs allows the computation of current flowing through an arbitrary monodimensional semiconductor structure in presence of light shining from the two sides. A good insight of the mechanism regulating the p-i-n structure behavior under the different illumination conditions of the experiment, can be gained from the calculated charge and recombination profiles. In Fig.3 the charge distribution within the i-layer for different illumination conditions is reported assuming a density of deep states of 5e15 [cm^{-3}]. Three zones are easily distinguished: two at the extrema of the structure, of variable thickness, a third one in the middle in which the charge is approximately constant at a value fixed by the relative importance of the two light intensities. The thickness of this zone remains fixed even though its position changes. Comparing this results with recombination profiles reported in Fig.4, one can still individuate the same three zones; moreover the central one is characterized by a level of recombination which is always negligible compared to the other two. Even though the relative extension of the zones is found to change for different choices of capture cross sections of dangling bonds, the structure itself, i.e. the presence of three well defined zones, remains the same.
The change in the position of the charged, central, zone with different illumination conditions, gives a possible explanation for the difference, experimentally found, between the saturated asymptotic values of collection (zones C1 and C2 of Fig.2). In presence of a non-homogeneous space distribution of dangling bonds with the maximum near the p-i interface, the charge stored when I_{bn} is predominant over I_{bp} is higher than the one accumulated when I_{bp} prevails on I_{bn}: this results in a larger electric field quenching and a lower measured collection.

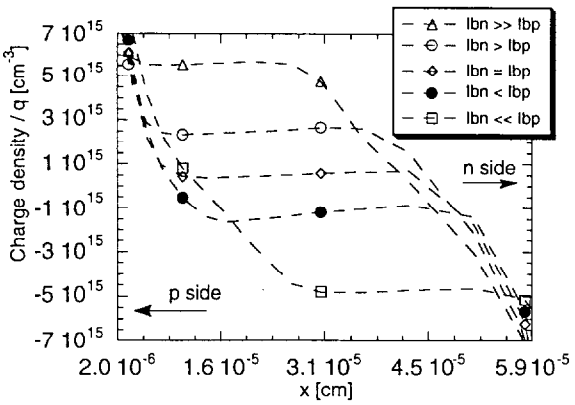

Fig.3: Charge distribution within the intrinsic layer of a p-i-n device under different blue light intensities, I_{bp} and I_{bn}, shining from p and n sides, respectively.

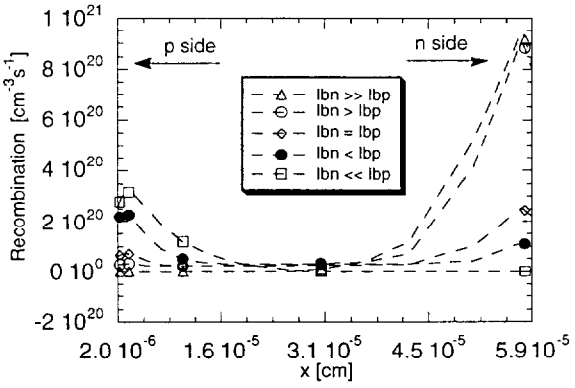

Fig.4: Recombination profiles within the intrinsic layer of a p-i-n device under different blue light intensities, I_{bp} and I_{bn}, shining from p and n sides, respectively

ANALYTICAL MODEL

The development of an analytical model can help one to explain experimental data on the basis of a small amount of parameters underlining, thus, in a non-ambiguous way the role played by each of the parameters in determining the device beahvior. On the other hand, it requires a simplified picture of complex mechanisms such as the ones which, in general, regulate photocurrent collection in an a-Si:H p-i-n device: the particular structure of the two blue beam experiment helps in drawing this picture.
Following the general behavior of charge distribution and recombination profiles, as can be seen from the numerical simulation, it seems justified to divide the intrinsic layer of the p-i-n cell into three zones. The thickness of the central zone is W and it can move within the intrinsic layer for different experimental conditions enlarging or collapsing the other two zones Continuity equations can be written for each zone, generation (G_1, G_2) and recombination (R_1 , R_2) taking place only in the outer zones, Fig.5.

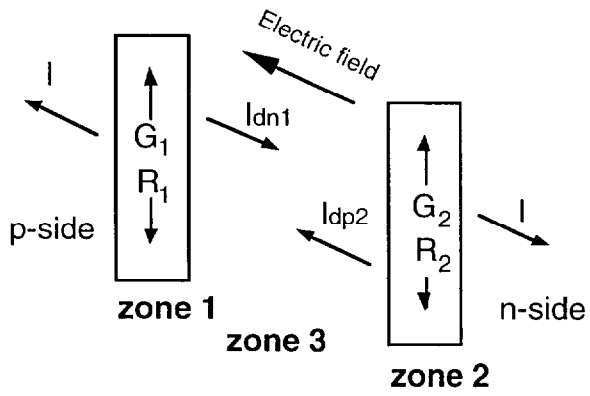

Fig.5: Three zones model for the intrinsic layer of the p-i-n cell.

At high reverse voltage, with unity collection, the photocurrent is given by

$$I_{rb} = (G_1 + G_2) * q \qquad (1),$$

where G_1 and G_2 are the generation currents, integrated all over zone 1 and 2 respectively, due to the light entering the p- and n- sides respectively.
At short circuit, neglecting diffusion currents, one obtains

$$I_{sc} = (G_1 + G_2 - R_1 - R_2) * q = I_{dn1} + I_{dp2} \qquad (2),$$

in which R_1 and R_2 are the total, integrated, recombination in zones 1 and 2 respectively. Eq.2 is the key point of the model: the assumption of a negligible level of recombination in zone three results in the possibility to solve the equations in term of the drift currents which flows there, thus avoiding the need for a description of the recombination terms in zone 1 and 2. Drift currents can be expressed as:

$$I_{dn1} = q\,\mu_n\,n_1\,E_0 \quad , \quad I_{dp2} = q\,\mu_p\,p_2\,E_w \qquad (3)$$

In which E_0 and n_1 (E_w, p_2) are the electric field intensities and the density of free electrons (holes) at the border between zone 1(2) and 3; μ_n and μ_p are band mobilities.
Electric field evolution in zone 3 is a linear function of the distance as the charge trapped there is assumed constant (Fig.3); the average value of the electric field multiplied by the zone thickness (W) gives the built-in voltage (V_{bi}).

$$E(x) = V_{bi} / W + S\,(W/2 - x) / \varepsilon \qquad (4)$$

Charge S is the charge trapped in the dangling bonds; non-homogeneity in the spatial distribution of dangling bonds, which, as noted in the discussion of the numerical simulation, results in an asymmetry of the maximum charge which can be stored under opposite condition of illumination, are taken into account by the offset term Q_o

$$S = Q_{db} + Q_o \qquad (5)$$

Charge trapped in dangling bonds can be related to the amount of photogenerated free carriers by [1]

$$Q_{db} = qN_{db}\left(\frac{p}{n}\frac{\sigma_p^0}{\sigma_n^+} - \frac{n}{p}\frac{\sigma_n^0}{\sigma_p^-}\right)\Bigg/\left(\frac{p}{n}\frac{\sigma_p^0}{\sigma_n^+} + 1 + \frac{n}{p}\frac{\sigma_n^0}{\sigma_p^-}\right) \qquad (6)$$

in which N_{db} is the average density of dangling bonds and $\sigma_{n,p}^{-,0,+}$ are their capture cross-sections for electrons and holes in different states of charge. Using eqs. 1-6, the internal collection, given by the ratio of the photocurrent at short circuit and at high reverse bias, is

$$\frac{I_{sc}}{I_{rb}} = \frac{\frac{V_{bi}}{W}\left(n_1\mu_n + p_2\mu_p\right) + \frac{SW}{2\varepsilon}\left(n_1\mu_n - p_2\mu_p\right)}{G_1 + G_2} \qquad (7).$$

Assuming a proportional relationship between generation and free carrier concentration at the borders of zone 3

$$G_1 = K_1\,n_1 \; ; \; G_2 = K_2\,p_2 \qquad (8)$$

and defining

$$X = G_2 / G_1 = K_2\,p_2 / K_1\,n_1 = I_{bn} / I_{bp} \qquad (9)$$

one obtains

$$\frac{I_{sc}}{I_{rb}} = \frac{\mu_n}{K_1}\frac{\frac{V_{bi}}{W}(1 + AX) + \frac{SW}{2\varepsilon}(1 - AX)}{1 + X} \qquad (10)$$

with

$$A = K_1\,\mu_n / K_2\,\mu_p \qquad (11)$$

Expressions for K1 (K2) can be found by evaluating the limit, while letting the p/n ratio go towards infinity (zero), for the continuity equations in zone 1 (2); in such a condition the electric field is strongly distorted, the thickness of the zone dramatically shrinks and the only contribution to the recombination current remains the interface recombination. Interface recombination is not dependent on the bulk density of states and can be assumed to be proportional to the minority carrier concentration via the 'surface' velocity S_v [2]

$$\lim_{p/n \to \infty} R_1 = \lim_{p/n \to \infty} G_1 - \frac{I_{dn1}}{q} = S_{r1} = n_1 S_{v1} \qquad (12)$$

from which

$$K_1 = \mu_n\left(\frac{V_{bi}}{W} + \frac{W}{2\varepsilon}\left(qN_{db} + Q_o\right)\right) + S_{v1} \qquad (13).$$

With a similar reasoning:

$$K_2 = \mu_p\left(\frac{V_{bi}}{W} + \frac{W}{2\varepsilon}\left(qN_{db} - Q_o\right)\right) + S_{v2} \qquad (14)$$

FIT OF EXPERIMENTAL DATA USING THE ANALYTICAL MODEL

The Levenberg-Marquardt algorithm [3] has been used to fit the analytical model to experimental data. The result is reported in Fig.6: the analytical model follows fairly well experimental data over five orders of magnitude of the abscissa. The parameters yielded by the fit procedure are reported in Tab.1 and Fig.7. All the experimental curves, as referring to different degradation stages, are fitted together: the number of dangling bonds (N_{db}) is the only quantity which is allowed to vary as a function of degradation time.

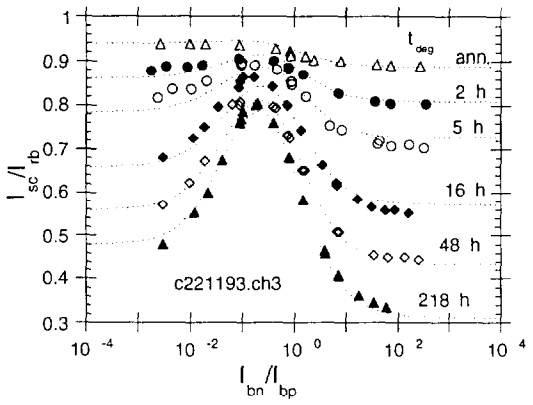

Fig.6. The analytical model fitted over experimental data: the fit of different degradation stages is obtained changing only the number of dangling bonds.

The determination of the absolute value of the deep density of defects (N_{db}) relies on the knowledge of the thickness of the zone 3 of the model (W). In the numerical simulation this thickness has been found to vary from 1/3 to 1/2 of the whole intrinsic layer thickness when using different capture cross section ratios for the dangling bonds. Moreover, W does not vary when one changes the number of dangling bonds, thus it can be assumed constant through the whole degradation process allowing the independent determination of the relative increase of N_{db}. In Fig.7 the evolution of N_{db} is reported as a function of degradation time; W is thereby assumed to be 1/3 of the intrinsic layer thickness. Assuming $\mu_n = 10$, $\mu_p = 1$ [$cm^2/(Vs)$] and $V_{bi} = 1.1$ [V], surface velocities of 22200 and 5520 [cm/s] are obtained for the p-i and i-n interfaces, respectively. from parameters 2 and 3. Parameter 4 indicates a non-homogeneity in the spatial dangling bonds distribution of around 50% of the average value (N_{db}). This can be originated by the non-uniform absorption profile of the light used for the degradation.
Finally, a value of around 3 for the capture cross section ratios of the dangling bonds (charged over neutral) can be deduced from parameters 5 and 6. This is surprisingly low [4] although it is still physically reasonable. As a first presentation of the method we stress the fact that still a large amount of work must be done in order to fully understand the effect of the assumptions, which are used in the analytical model, on the specific values of parameters obtained by curve fitting. This is true, in particular, for the capture cross section ratios.

Parameter	Value
1) $qN_{db}W^2 / 2\varepsilon V_{bi}$	(see Fig.7)
2) $S_{v1}W / \mu_n V_{bi}$	0.037
3) $S_{v2}W / \mu_p V_{bi}$	0.092
4) Q_o / qN_{db}	0.46
5) $\mu_n\sigma^0{}_p / \mu_p\sigma^+{}_n$	3.3
6) $\sigma^0{}_n\sigma^0{}_p / \sigma^-{}_p\sigma^+{}_n$	0.09

Tab.1. Parameters of the analytical model and their values obtained by the fit of experimental data

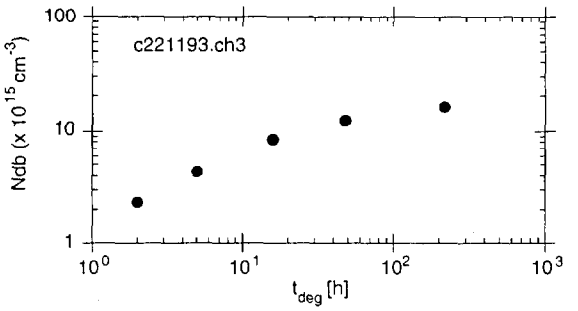

Fig.7. Density of dangling bonds as a function of the degradation time.

CONCLUSIONS

The collection of two sides blue light is shown to be an interesting tool for monitoring p-i-n solar cell degradation. The simple set-up used allows to probe the collection over a wide range of photocarrier populations, and thus yields a very detailed response of the solar cell operation as a function of degradation.
Experimental data is analized based on an analytical model, and the number of danglind bonds during degradation is estimated. The good agreement obtained between theory and experiment confirms the important role played by the dangling-bond charge state and its effect on the electric field shape in the amorphous silicon p-i-n solar cell. The detailed effect of model assumptions on the specific values of the fitted parameters requires, however, further investigation.

ACKNOWLEDGEMENTS

The great assistance of Sebastian Dubail is gratefully acknowledged for preparation of the samples. This work has been supported by Swiss research grant OFEN-REN93/032.

REFERENCES

[1]. J. Hubin, A.V.Shah and E. Sauvain *Phil. Mag. Lett.* **66**,p. 115,(1992)
[2]. S.M. Sze 'Physics of Semiconductor Devices' Wiley p.56
[3] W.H.Press et al.; 'Numerical Recipes', p.521, Cambridge, (1988)
[4] N. Wyrsch, A. Shah *J. Non-Cryst. Sol.* **137&138,** p. 431, (1991)